Electrostatic interaction between a rod-like macromolecule and a circular orifice/disk in an electrolyte solution*

Lian Zeng-Ju(连增菊)†

Department of Physics, Ningbo University, Ningbo 315211, *China*

(Received 7 December 2010; revised manuscript received 29 January 2011)

We present the solutions of the interaction energy for a colloid system with a charged rod-like macromolecule immersed in a bulk electrolyte and moving along the axis of a circular orifice or disk (orifice/disk). The calculation requires a numerical computation of the surface charge profiles, which result from a constant surface potential on the macromolecule and the orifice/disk. In the calculation, remarkable divergences of the surface charge emerge on the edges of the macromolecule and the orifice/disk, which are well-known edge effects. The anisotropic distribution of the surface charge (effective dipole) results in an attraction between these two charged objects. This attraction is enhanced with the increase of the screening length of the system for both the orifice and the disk systems. However, the sizes of the orifice and the disk reduce to different effects on the interaction energy.

Keywords: electrostatic interaction, Green's function, anistropic distribution

PACS: 64.70.pv, 47.57.J–, 41.20.Cv **DOI:** 10.1088/1674-1056/20/7/076401

1. Introduction

Nowadays, many experiments show that the electrostatic interaction between charged colloids and charged interfaces (charged membrane, ion–water interface, porous medium, etc.) plays one of the major roles in determining the physical properties of many aqueous colloidal suspensions.[1−6] The effect of the presence of a planar solid boundary was first examined theoretically by Morrison and Stukel[7] in a study on a hard particle, which was re-examined later by Keh *et al.*[8] with some mistakes corrected. The electrostatic interaction of colloidal spheres at some fixed boundaries, such as in a long circular tube and along the centreline between two large parallel plates, has also been theoretically studied under the assumption of infinitely thin double layers in Refs. [9] and [10]. However, a system possessing much more complex boundaries, such as a colloidal suspension with a porous boundary (membrane), is seldom considered. In addition, in the colloid world, a spherical shape is not the exclusive shape, many macromolecules are intrinsically very anistropic with rod-like or ribbon-like shapes (DNA molecules, TMV or fd virus, V_2O_5 ribbons, Boehmite rods, etc.)[11,12] and disk-like shapes (laponite, bentonite, etc.).[13,14] Coming back to basic ingredients, the electrostatic interaction between a moderately anisotropic colloid and a charged fixed boundary should therefore be specifically considered. In this paper, we investigate the electrostatic interaction between a charged circular orifice or disk and a charged rod-like macromolecule that creeps along the axis of the circular orifice or disk.

2. Model and theory

We consider a single charged rod-like macromolecule immersed in an electrolyte solution with a dielectric constant ϵ and moving along the axis of a circular orifice/disk (see Fig. 1). Within the framework of the Linear Poisson–Boltzmann (LPB) theory, the electric potential outside the macromolecule in the symmetric 1 : 1 electrolyte satisfies

$$\nabla^2\Phi(\boldsymbol{r}) = -\rho_{\rm f} = \kappa_{\rm D}^2\Phi(\boldsymbol{r}), \tag{1}$$

where $\rho_{\rm f}$ is the space charge density of the free ions and $\kappa_{\rm D} = \sqrt{2c_0\lambda_{\rm B}}$ denotes the Debye screening pa-

*Project supported by the Scientific Research Fund of the Education Department of Zhejiang Province of China (Grant No. Y200803420), the National Natural Science Foundation of China (Grant No. 10947175), the Natural Science Foundation of Ningbo, China (Grand No. 2010A610089), and K. C. Wong Magna Fund in Ningbo University of China.

†Corresponding author. E-mail: lianzengju@nbu.edu.cn

© 2011 Chinese Physical Society and IOP Publishing Ltd

rameter with $\lambda_{\rm B} = e^2\beta/\epsilon$ and $\beta = 1/k_{\rm B}T$. Here, e is the charge of an electron, c_0 is the average density of ions and $k_{\rm B}$ is the Boltzmann constant. The boundary conditions on the molecule and on the orifice/disk surfaces are

$$\Phi(\boldsymbol{r}) = \Phi_0, \quad \boldsymbol{r} \in \Sigma_i, \quad i = 1, 2. \tag{2}$$

Note that we assume that there is no charge inside the macromolecule (denoted by C in Fig. 1), i.e., $\Phi(\boldsymbol{r}) = \Phi_0$ for any point $\boldsymbol{r}$ inside the macroion (therefore $\Delta\Phi(\boldsymbol{r}) = 0$).

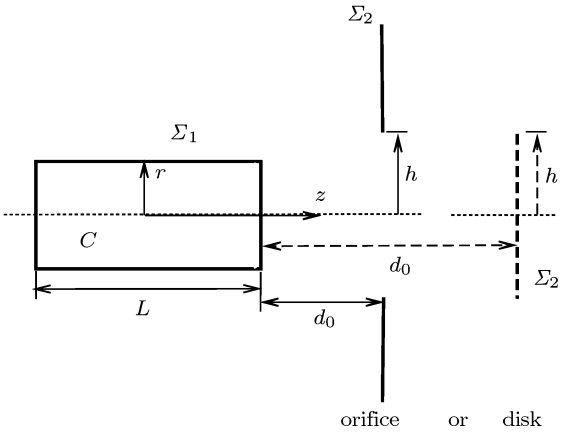


Fig. 1. A sketch of the system under consideration. A charged rod-like macromolecule C moves along the axis of a circular orifice or disk. These two charged objects are both immersed in an electrolyte solution.

The potential of the system can be obtained by solving Eqs. (1) and (2) through applying the standard Green's function. However, this task is too cumbersome due to the existence of a nonvanishing excluded region for the microions (inside the macromolecule), for which the LPB equation does not hold. Fortunately, this problem can be circumvented by applying an auxilary method introduced by Chapot *et al.*[15]

Following the Chapot method, we introduce an auxilary system, in which the LPB equation holds everywhere in the volume,

$$\begin{cases} \nabla^2\Phi'(\boldsymbol{r}) = \kappa_{\rm D}^2\Phi'(\boldsymbol{r}), & \text{any } \boldsymbol{r}, \\ \Phi'(\boldsymbol{r}) = \Phi_0, & \boldsymbol{r} \in \Sigma_i,\ i = 1, 2. \end{cases} \tag{3}$$

The corresponding auxilary surface charge densities on the macromolecule and on the orifice/disk, $\tilde{\sigma}_1$ and $\tilde{\sigma}_2$, are determined in terms of the solution of the previous system

$$\tilde{\sigma}_i(\boldsymbol{r}) = \epsilon_i^- \left(\frac{\partial\Phi'(\boldsymbol{r})}{\partial \boldsymbol{n}_i}\right)_{\Sigma_i^-} - \epsilon_i^+ \left(\frac{\partial\Phi'(\boldsymbol{r})}{\partial \boldsymbol{n}_i}\right)_{\Sigma_i^+}, \quad i = 1, 2, \tag{4}$$

where $\boldsymbol{n}_i$ is the outward pointing normal unit vector of surface Σ_i, ϵ_i^+ and ϵ_i^- are dielectric constants of surfaces Σ_i^+ and Σ_i^-, respectively. Now, the solution of Eq. (3) can be easily determined in terms of the surface charge densities $\tilde{\sigma}_1$ and $\tilde{\sigma}_2$,

$$\Phi'(\boldsymbol{r}) = \iint_{\Sigma_1} \tilde{\sigma}_1(\boldsymbol{r}')G(\boldsymbol{r}, \boldsymbol{r}')\,{\rm d}S' + \iint_{\Sigma_2} \tilde{\sigma}_2(\boldsymbol{r}')G(\boldsymbol{r}, \boldsymbol{r}')\,{\rm d}S', \tag{5}$$

where $G(\boldsymbol{r}, \boldsymbol{r}')$ is the Green's function, $G(\boldsymbol{r}, \boldsymbol{r}') = {\rm e}^{-\kappa_{\rm D}|\boldsymbol{r}-\boldsymbol{r}'|}/(4\pi\epsilon|\boldsymbol{r}-\boldsymbol{r}'|)$, which describes the potential at point $\boldsymbol{r}$ created by a unit point charge at position $\boldsymbol{r}'$. The unknown auxiliary charge densities, $\tilde{\sigma}_1$ and $\tilde{\sigma}_2$, can be determined by imposing the boundary conditions on the macromolecule and the orifice/disk,

$$\iint_{\Sigma_1} \tilde{\sigma}_1(\boldsymbol{r}')G(\boldsymbol{r}, \boldsymbol{r}')\,{\rm d}S' + \iint_{\Sigma_2} \tilde{\sigma}_2(\boldsymbol{r}')G(\boldsymbol{r}, \boldsymbol{r}')\,{\rm d}S' = \Phi_0, \quad \boldsymbol{r} \in \Sigma_i, \quad i = 1, 2. \tag{6}$$

The overall result of these general considerations is a formal solution of the LPB Eq. (1), $\Phi(\boldsymbol{r})$, for any point outside the macromolecule.

To obtain the real charge densities on the surfaces of the macromolecule and the orifice/disk, we need to compute the surface charge densities each as a function of the auxiliary $\tilde{\sigma}$ by using the definition

$$\sigma_1(\boldsymbol{r}) = -\epsilon \left(\frac{\partial\Phi(\boldsymbol{r})}{\partial \boldsymbol{n}_1}\right)_{\Sigma_1^+}$$
$$\sigma_2(\boldsymbol{r}) = \epsilon \left[\left(\frac{\partial\Phi(\boldsymbol{r})}{\partial \boldsymbol{n}_2}\right)_{\Sigma_2^-} - \left(\frac{\partial\Phi(\boldsymbol{r})}{\partial \boldsymbol{n}_2}\right)_{\Sigma_2^+}\right], \tag{7}$$

where $\Phi(\boldsymbol{r})$ is the solution of Eqs. (1) and (2), and equals $\Phi'(\boldsymbol{r})$ outside the macromolecule.

3. Charge distributions on the particle and on the orifice/disk

3.1. Sketch of the numerical method

According to the introduction in Section 2, to obtain the real surface charge of the system, we should start with the computation of the auxiliary surface charge density by inverting Eq. (6). This calculation involves the screened electrostatic Green's function, which was introduced in the previous section. A numerical calculation needs to be performed to compute the inverse matrix of $G(\boldsymbol{r}, \boldsymbol{r}')$ on the (discretized)

macroion and on the orifice/disk. Due to the cylindrical symmetry of the problem, we can reduce the dimensionality of the problem by integrating the Green's function over a ring (or small cylinder) that has its centre matched with the axis of symmetry of the cylinder, as illustrated in Fig. 2. Then, the cylinder C and the orifice/disk surfaces Σ_2 can be decomposed into the superposition of small cylinders (on the lateral surface) and rings (on the head surfaces and on the orifice/disk surface) denoted as C_j and R_i or D_k (on the orifice/disk surface) with dimension l and surface charge density $\tilde{\sigma}_{1,i}$ or $\tilde{\sigma}_{2,i}$ (on the orifice/disk surface). Finally, equation (6) can be discretized as follows:

$$\sum_{i}^{\boldsymbol{r}_i\in\Sigma_1}\tilde{\sigma}_{1,i}G_i(\boldsymbol{r}_i,\boldsymbol{r}_j)+\sum_{i}^{\boldsymbol{r}_i\in\Sigma_2}\tilde{\sigma}_{2,i}G_i(\boldsymbol{r}_i,\boldsymbol{r}_j)=\Phi_0,\quad \boldsymbol{r}_j\in\Sigma_k,\quad k=1,2, \tag{8}$$

where $G_i(\boldsymbol{r}_i,\boldsymbol{r}_j)$ is the electrostatic potential created on the cylinder C_j, ring R_j or D_j by the cylinder C_i, ring R_i or D_i carrying a unit surface charge density. These expressions can be easily obtained from the derivatives of the potential created by a disk, which can be found in Ref. [16]. We denote the potential created by an elementary ring and an elementary cylinder as $G_{\rm ring}$ and $G_{\rm cyl}$, respectively. A more detailed description is given in Appendix A. Once the corresponding reduced Green's function is known, the numerical task is simplified into a standard inversion problem. The real surface charge densities σ_1 and σ_2 can be deduced from the obtained auxiliary surfaces charge densities $\tilde{\sigma}_1$ and $\tilde{\sigma}_2$ through using Eq. (7). The discretized forms read

$$\begin{aligned}
&\sigma_1(\boldsymbol{r}_j)\\
&=-\epsilon\sum_{i}^{\boldsymbol{r}_i\in\Sigma_1}\tilde{\sigma}_{1,i}\frac{\partial G_i(\boldsymbol{r}_i,\boldsymbol{r}_j)}{\partial\boldsymbol{n}_{1,j}}-\epsilon\sum_{i}^{\boldsymbol{r}_i\in\Sigma_2}\tilde{\sigma}_{2,i}\frac{\partial G_i(\boldsymbol{r}_i,\boldsymbol{r}_j)}{\partial\boldsymbol{n}_{1,j}},\\
&\quad j\in\Sigma_1^+,\\
&\sigma_2(\boldsymbol{r}_j)\\
&=\epsilon\left[\sum_{i}^{\boldsymbol{r}_i\in\Sigma_1}\tilde{\sigma}_{1,i}\frac{\partial G_i(\boldsymbol{r}_i,\boldsymbol{r}_j)}{\partial\boldsymbol{n}_{2,j}}+\sum_{i}^{\boldsymbol{r}_i\in\Sigma_2}\tilde{\sigma}_{2,i}\frac{\partial G_i(\boldsymbol{r}_i,\boldsymbol{r}_j)}{\partial\boldsymbol{n}_{2,j}}\right]\\
&\quad-\epsilon\left[\sum_{i}^{\boldsymbol{r}_i\in\Sigma_1}\tilde{\sigma}_{1,i}\frac{\partial G_i(\boldsymbol{r}_i,\boldsymbol{r}_k)}{\partial\boldsymbol{n}_{2,k}}+\sum_{i}^{\boldsymbol{r}_i\in\Sigma_2}\tilde{\sigma}_{2,i}\frac{\partial G_i(\boldsymbol{r}_i,\boldsymbol{r}_k)}{\partial\boldsymbol{n}_{2,k}}\right],\\
&\quad j\in\Sigma_2^-,\quad k\in\Sigma_2^+,
\end{aligned} \tag{9}$$

where G_i takes either the cylinder form or the ring form obtained in Eqs. (A3) or (A4) in Appendix A, respectively.

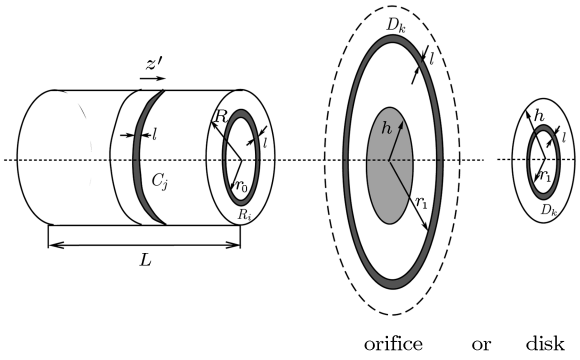


Fig. 2. During the numerical calculations, the cylinder and the orifice/disk are decomposed into small cylinders C_j and small rings, R_i and D_k. Each of these elementary surfaces carries a uniform surface charge density $\tilde{\sigma}_{1,i}$ or $\tilde{\sigma}_{2,i}$ (on the orifice/disk). The numerical calculations are performed with $l\leq 0.05l_{\rm D}$.

3.2. Numerical results

We now present the results of the surface charge densities on the lateral and on the heads of the cylinder and on the orifice or disk, which are denoted as $\sigma_{\rm cyl}(z)$, $\sigma_{\rm head}(r)$ and $\sigma_{\rm ori}(r)$ or $\sigma_{\rm disk}(r)$, respectively.

Typical results for the profiles of the surface charge on the lateral of the cylinder are shown in Fig. 3. To facilitate the comparison, we also plot the free ion density $\rho_{\rm f}$. From Fig. 3, we find that there are striking divergences of the surface charge profiles close to the edge of the lateral of the cylinder for both the orifice and the disk systems. This is the well know edge effect, which is expected for charged object with a uniform potential. In the absence of the electrolyte ($\kappa_{\rm D}=0$), the divergence of the surface charge in the vicinity of the edge is a classical result.[17] For an infinite conducting dielectric with an edge angle α, the surface charge density σ is found to diverge in the vicinity of the edge as $\rho^{\pi/\alpha-1}$, where ρ is the distance to the edge. For a cylinder, corresponding to $\alpha=3\pi/2$, the surface charge is expected to diverge as $\rho^{-1/3}$. In an electrolyte, i.e., $\kappa_{\rm D}\neq 0$, the case is obviously more complex. However, the divergence is expected to remain. Additionally, in the centre area of the lateral, the charge distributes uniformly as the reduced centre–centre distance between the macromolecule and the orifice/disk d/R increases, while they change almost linearly with z/R as the d/R decreases.

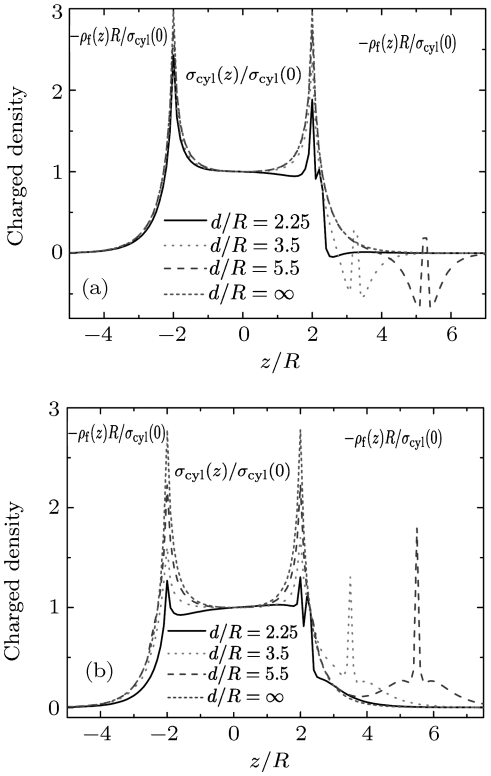


Fig. 3. Variations of reduced surface charge on the lateral of the cylinder $\sigma_{cyl}(z)/\sigma_{cyl}(0)$ with z/R for: (a) the orifice system and (b) the disk system. The reduced free ion density $-\rho_f(z)R/\sigma_{cyl}(0)$ is also plotted for comparison. The aspect ratio of the cylinder L/R is 4, the reduced radius of the orifice/disk h/R is 1.5, and the screening factor $\kappa_D R$ is 0.583.

Figures 4 and 5 show that the profiles of the surface charge on the cylinder head and on the orifice/disk also exhibit edge effects. Furthermore, due to the effect of the charged orifice/disk with uniform potential, the surface charge peak location on the cylinder head shifts toward the centre as the macromolecule gets closer to the orifice/disk. This phenomenon vanishes rapidly when the macromolecule leaves along the axis of the orifice/disk for both the orifice and the disk systems. At the same time, the profiles of the surface charge on the orifice/disk are affected by the macromolecule with uniform potential. Especially for the disk system, a peak in the surface charge profile emerges at the ratio of $r/R = 1.0$ when the molecule and the disk are close (such as $d/R = 2.25$, see Fig. 5). Finally, it is interesting to compare the profiles with that of the edge effect divergence predicted for the $\kappa_D = 0$ limit. Only the charge profile on the head of the cylinder is found to be in semi-quantitative agreement with the scaling law, as shown in Fig. 4. This is expected. Since in our calculation, the length L of the cylinder is larger than the Debye length κ_D^{-1} and the radius of the cylinder R is much smaller than κ_D^{-1}, then the $\kappa_D = 0$ profile is only a very crude approximation to that of the lateral surface, while it is a fair but not bad approximation to that of the head surface.

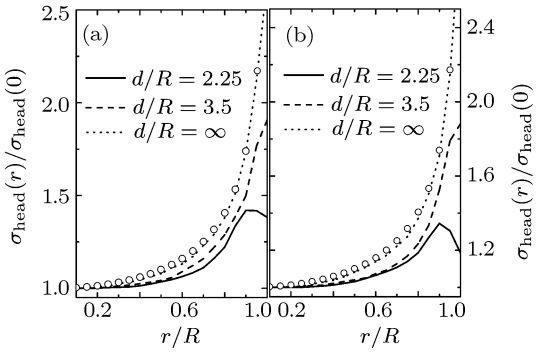


Fig. 4. Variations of the reduced surface charge on the head of the cylinder with r/R for: (a) the orifice system and (b) the disk system. The other parameters are the same as those in Fig. 3. The predicted scaling for the divergence in the absence of electrolyte ($\kappa_D R = 0$), $\sigma_{head}(r)/\sigma_{head}(0) = [1-(r/R)^2]^{-1/3}$, is also plotted (denoted by circles).

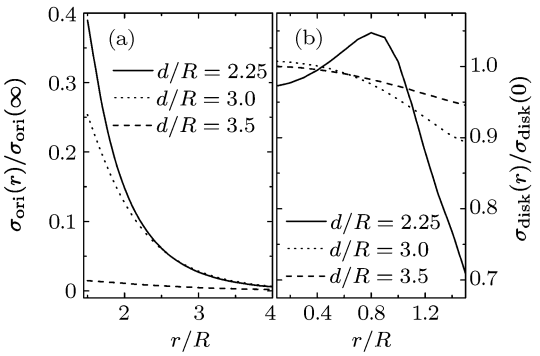


Fig. 5. Variations of the surface charge on the surfaces of (a) the orifice and (b) the disk.

4. Interaction energy of the charged macromolecule and the charged orifice/disk

Under the linear approximation, the interaction energy between the macromolecule and the orifice/disk can be written as a sum of surface integrals over the cylinder and the orifice/disk[18]

$$\beta\Omega = \frac{1}{2}\left(\iint_{\Sigma_1} \mathrm{d}S\sigma_1(\boldsymbol{r})\Phi(\boldsymbol{r}) + \iint_{\Sigma_2} \mathrm{d}S\sigma_2(\boldsymbol{r})\Phi(\boldsymbol{r}) \right) - \beta\Omega_0, \quad (10)$$

where Ω_0 is determined by solving the LPB problem with an infinite distance between the particle and the

orifice/disk. The potential outside the macromolecule $\Phi(\boldsymbol{r})$ can be found directly with Eq. (5) once the auxiliary charge density $\tilde{\sigma}$ is obtained.

We now focus on the interaction energy varying with the reduced particle-orifice/disk distance d/R with different values of reduced orifice/disk radius h/R. From Fig. 6, we can find that there is an electrostatic attraction between the particle and the orifice/disk (electrostatic force $F \propto -\partial\Omega/\partial d$). This attraction is due to the interaction between the effective electric dipoles of the particle and of the orifice/disk, which come from the anisotropies of the surface charge on these charged objects. Based on the profiles of the surface charge shown in Figs. 3–5, the effective dipole vectors can be indicated, as shown in Fig. 6. The effective dipole vector on the head of the cylinder points to the centre, while the dipole vector of the orifice/disk is in the opposite direction. This obviously causes an attraction. Similarly, the electrostatic attraction between the like-charge macromolecules has also been reported by Pillips[19] both in theory and in experiment. An anomalous long-range attractive interaction between two like-charge colloids confined in a conducting plane was also found by Grier and Han.[20] All of those are not strongly accounted for by the Derjaguin–Landau–Verwey–Overbeek theory.[21,22] Additionally, Trizac and Derjaguin,[23] Sader *et al.*[24] have shown that within the Poisson-Boltzmann (PB) theory, no like-charge attraction is possible. However, none of them considered the anisotropy of the surface charge in their studies. In fact, the distribution of the surface charge affects the electrostatic interactions quantitatively and qualitatively, which has also been confirmed in our previous work.[18,25]

Meanwhile, the sizes of the orifice/disk h/R also affect the interactions strongly. This is confirmed when h/R is varied. For the orifice system, the amplitude of the electrostatic interaction energy decreases with the increase of the reduced orifice radius h/R at a small colloid–orifice distance. Of course, the interaction energy vanishes when $h/R \sim \infty$ (see the dash line in Fig. 6(a)), and reaches the largest when the reduced orifice radius $h/R = 0$ (see the solid line in Fig. 6(a)). In the latter situation, the orifice becomes a plane. The situation is much different for that of the disk system. The interaction energy increases with the increase of the reduced disk radius h/R. When the disk radius h/R approaches to ∞, the disk also becomes a plane (the result is shown as solid line in Fig. 6(b)).

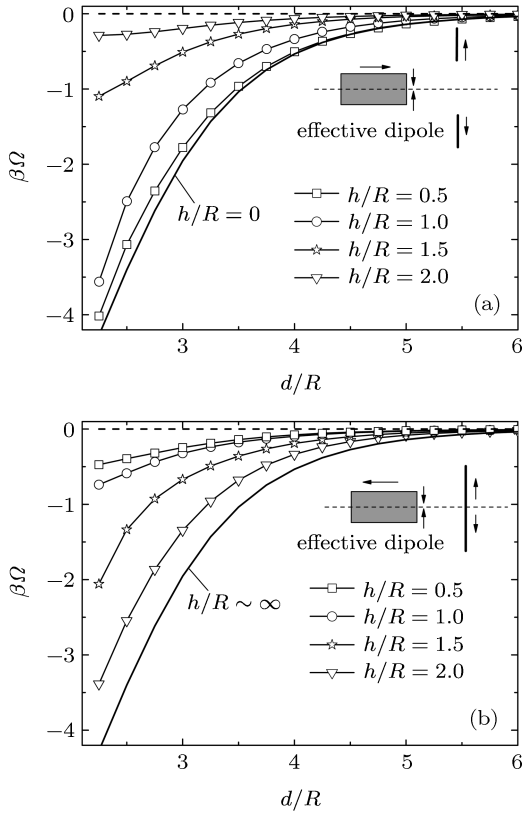


Fig. 6. The reduced interaction energy of the rod-like charged macromolecule and the charged (a) orifice or (b) disk versus the reduced centre–centre distance of these two objects. The aspect ratio $L/R = 4$ and the screening factor $\kappa_{\rm D}R = 1.183$.

Figure 7 shows the results of the interaction energy with different values of reduced screening factor $\kappa_{\rm D}R$. Compared with the bigger $\kappa_{\rm D}R$, the smaller one tends to enhance the interaction. This phenomenon can also be found in a spherical macromolecule system and a bulk system with rod colloids.[15,25] Additionally, for

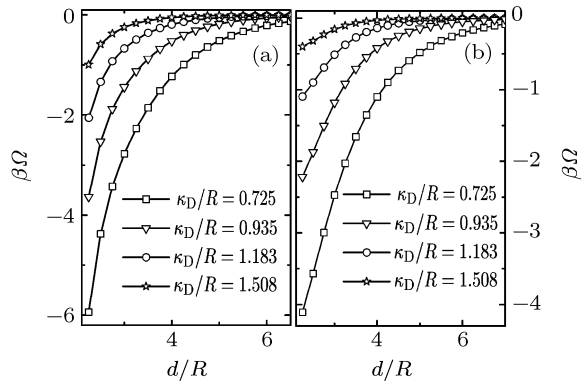


Fig. 7. The reduced interaction energy of the rod-like charged macromolecule and the charged (a) orifice or (b) disk versus the reduced centre–centre distance of these two objects for difference screening factor $\kappa_{\rm D}R$. The reduced radius of the orifice/disk is $h/R = 1.5$.

a general colloid solution, the Debye screening parameter is expressed as $\kappa_{\rm D}^2 = \lambda_{\rm B} \sum n_i z_i$, with n_i the concentration of the i-th ionic species in the solution and z_i the corresponding valence. Hence, we can change the interaction between the colloid and the charged boundaries by changing the concentrations and the valences of the salt ions in experiment.

5. Conclusion

In the present paper, we investigate a colloid system of a charged rod-like macromolecule with a finite aspect ratio immersed in a bulk electrolyte and moving along the axis of a circular orifice or disk. In the linear Poisson–Boltzmann framework, we calculate the interaction energy of the macromolecule and the orifice/disk. An auxiliary surface charge density $\tilde{\sigma}$ is introduced during solving the LPB equation. This auxiliary surface charge density can be found by inverting the boundary conditions on the macromolecule and on the orifice/disk surface. As the auxiliary surface charge density is obtained, the other physical quantities, such as the real charge density σ, the potential of the system Φ and the interaction energy, can be obtained by computing the functions of the auxiliary quantity $\tilde{\sigma}$.

The calculation results of the real surface charge indicate that there are remarkable divergences on the edges of the particle and of the orifice/disk. The edge effects are due to the uniform potential conditions on the surfaces of these charged objects. In the absence of an electrolyte ($\kappa_{\rm D} = 0$), the divergence of the surface charge in the vicinity of the edge is a classical result. Obviously, it is still valid for the charged object embedded in an electrolyte, though the situation is more complex. In addition, the profiles of the surface charge of one charged object, such as the colloid, are simultaneously disturbed by the other charged object with uniform surface potential, such as the orifice/disk.

The anisotropic distribution of the surface charge (effective dipoles) results in an electrostatic attraction between two charged objects. This attraction is enhanced as the particle approaches the orifice/disk. The result may be helpful for understanding many phenomena in experiment, such as the absorbtion of charged colloids on a membrane in various fields[2,26] and the increase of the velocity of a charged colloid as it approaches an orifice in an experiment of colloid electrophoresis.[27] Furthermore, the sizes of the orifice/disk and the screening length of the system are other crucial ingredients for this interaction.

Appendix A: Reduced Green's function

The electrostatic potential created by a disk with radius R at point M in cylindrical coordinates $\{r, z\}$ (the origin being placed at the centre of the disk) reads

$$G_{\rm disk}(R, r, z) = \frac{R}{2\epsilon} \int_0^\infty \frac{{\rm J}_1(kR){\rm J}_0(kr)}{\sqrt{k^2 + \kappa_{\rm D}^2}} \times \ {\rm e}^{-\sqrt{k^2+\kappa_{\rm D}^2}|z-z'|} {\rm d}k, \qquad \text{(A1)}$$

where $\rm J_0$ and $\rm J_1$ are the Bessel functions of orders 0 and 1, respectively. The disk carrying a uniform surface charge (here equal to unity) is immersed in an electrolyte with Debye length $l_{\rm D}$ and is locate at height z'. The potential ${\rm d}G_{\rm cyl}(R, r, z)$ created at point M by an infinitesimal cylinder with height ${\rm d}z'$, radius R and unit surface charge can be obtained directly as

$${\rm d}G_{\rm cyl}(R, r, z) = {\rm d}z' \frac{\partial G_{\rm disk}(R, r, z)}{\partial R}. \qquad \text{(A2)}$$

As a result, the electrostatic potential created by a cylinder of radius R, height l and unit surface charge with the centre located at $(0, z')$ is given by

$$G_{\rm cyl}(R, z', r, z) = \frac{R}{2\epsilon} \int_{z'-l/2}^{z'+l/2} {\rm d}z'' \int_0^\infty \frac{k{\rm J}_0(kr){\rm J}_0(kR)}{\sqrt{k^2 + \kappa_{\rm D}^2}} \times \ {\rm e}^{-\sqrt{k^2+\kappa_{\rm D}^2}|z-z''|} {\rm d}k. \qquad \text{(A3)}$$

Along the same lines, the potential $G_{\rm ring}(r_0, r, z)$ created by a ring with radius r_0 and thickness l can be expressed in terms of $G_{\rm disk}(r_0, r, z)$ as

$$G_{\rm ring}(r_0, r, z) = G_{\rm disk}(r_0 + l/2, r, z) - G_{\rm disk}(r_0 - l/2, r, z). \qquad \text{(A4)}$$

References

[1] Buyukdagli S, Manghi M and Palmeri J 2010 *Phys. Rev.* E **81** 041601
[2] Lee S W, Park S E and Park S J 2007 *J. Ind. Eng. Chem.* **13** 395
[3] Chen W, Tan S, Huang Z, Ng T K, Ford W T and Tong P 2006 *Phys. Rev.* E **74** 021406
[4] Zhang L F and Huang J P 2010 *Chin. Phys.* B **19** 024213
[5] Guo J Y, Huang L X and Xiao C M 2006 *Chin. Phys.* B **15** 1638
[6] Hilal N, Ogunbiyl O O, Miles N J and Nigmatullin R 2005 *Sep. Sci. Technol.* **40** 1957
[7] Morrison F A and Stukel J J 1970 *J. Colloid Interface Sci.* **33** 88
[8] Keh H J, Lien L C and Chin J 1989 *Inst. Chem. Engin.* **20** 283

[9] Keh H J and Anderson J L 1985 *J. Fluid Mech.* **194** 417
[10] Keh H J and Lien L C 1991 *J. Fluid Mech.* **224** 305
[11] Purdy K R, Dogic Z, Fraden S, Rühm A, Lurio L and Mochrie S G J 2003 *Phys. Rev.* E **67** 031708
[12] Chen Y F, Milstein J N and Meiners J 2010 *Phys. Rev. Lett.* **104** 258103
[13] Shayeganfar F, Farouji S J, Movahed M S, Jafari G R and Tabar M R 2010 *Phys. Rev.* E **81** 061404
[14] van der Beer D and Lekkerkerker H N W 2003 *Europhys. Lett.* **61** 702
[15] Chapot D, Bocquet L and Trizac E 2004 *J. Chem. Phys.* **120** 3969
[16] Leote de Carvalho R J F, Trizac E and Hansen J P 2000 *Phys. Rev.* E **61** 1634
[17] Jackson J D 1975 *Classical Electrodynamics* (New York: Wiley)
[18] Lian Z J and Ma H R 2007 *J. Chem. Phys.* **127** 104507
[19] Phillips R J 1995 *J. Colloid Interface Sci.* **175** 386
[20] Grier D G and Han Y 2007 *Phys. Rev.* E **76** 041406
[21] Derjaguin B V and Landau L D 1994 *Acta Physicochim* **14** 733
[22] Verwey E J W and Overbeek J T G 1948 *Theory of Stability of Lyophobic Colloids* (Amsterdam: Elsevier)
[23] Trizac E and Raimbault J L 1999 *Phys. Rev.* E **60** 6530
[24] Sader J E, Derek Y and Chan C 1999 *J. Colloid Interface Sci.* **213** 268
[25] Lian Z J and Ma H R 2008 *J. Phys. Condens. Matter* **20** 035109
[26] Baker R W 2004 *Membrane Technology and Applications* 2nd edn. (Chichester: John Wiley & Sons)
[27] Keh H J and Lien L C 1991 *J. Fluid Mech.* **224** 305